















MaNGA 8313-1901: gas accretion observed in a blue compact dwarf galaxy?

MENGTING JU (居梦婷) ^{1,2} JUN YIN (尹君) ^{1,3} RONGRONG LIU (刘蓉蓉) ^{1,2} LEI HAO (郝蕾) ¹
ZHENGYI SHAO (邵正义) ^{1,3} SHUAI FENG (冯帅) ^{4,5} ROGÉRIO RIFFEL ^{6,7} CHENXU LIU (刘辰旭) ⁸
DAVID V. STARK ^{9,10} SHIYIN SHEN (沈世银) ^{1,3} EDUARDO TELLES,¹¹ JOSÉ G. FERNÁNDEZ-TRINCADO ¹²
JUNFENG WANG (王俊峰) ¹³ HAIGUANG XU (徐海光),¹⁴ DMITRY BIZYAEV ^{15,16} AND YU RONG (容昱) ¹⁷

ABSTRACT

Gas accretion is an important process in the evolution of galaxies, but it has limited direct observational evidences. In this paper, we report the detection of a possible ongoing gas accretion event in a Blue Compact Dwarf (BCD) galaxy, MaNGA 8313-1901, observed by the Mapping Nearby Galaxies and Apache Point Observatory (MaNGA) program. This galaxy has a distinct off-centered blue clump to the northeast (the NE clump) that shows low metallicity and enhanced star-formation. The kinematics of the gas in the NE clump also seems to be detached from the host BCD galaxy. Together with the metallicity drop of the NE clump, it suggests that the NE clump likely has an external origin, such as the gas accretion or galaxy interaction, rather than an internal origin, such as an H II complex in the disk. After removing the underlying host component, we find that the spectrum of the “pure” clump can match very well with a modeled spectrum containing a stellar population of the young stars (≤ 7 Myr) only. This may imply that the galaxy is experiencing an accretion of cold gas, instead of a merger event involving galaxies with significant pre-existing old stars. We also find signs of another clump (the SW clump) at the south-west corner of the host galaxy, and the two clumps may share the same origin of gas accretion.

arXiv:2209.03298v1 [astro-ph.GA] 7 Sep 2022

MaNGA 8313-1901 = SDSS J160108.90+415250.7	
Parameters	Data
MaNGA ID	1-248352
RA (J2000)	16:01:08.90 (240.28712°)
DEC (J2000)	+41:52:50.77 (41.88075°)
z^a	0.02425
d [Mpc]	103.932
M_{NUV} [mag] ^a	-17.46
M_g [mag] ^a	-18.64
M_r [mag] ^a	-18.86
M_z [mag] ^a	-19.03
$\log(M_*/M_\odot)^a$	8.88
$\log(M_*/M_\odot)^b$	9.28
$\log(M_{\text{HI}}/M_\odot)^c$	9.37
$\log(M_{\text{halo}}/M_\odot)^d$	11.03
seraic index ^e	1.46 ± 0.04 (the host galaxy) 0.19 ± 0.04 (the NE clump)
effective radius ^e [kpc]	1.23 ± 0.13 (the host galaxy) 0.29 ± 0.01 (the NE clump)

^a The NASA-Sloan Atlas catalog: <http://www.nsatlas.org>

^b The MPA - JHU catalog (Kauffmann et al. 2003a)

^c Masters et al. (2019)

^d Yang et al. (2007, 2012)

^e See more details in Section 3

Table 1. Properties of MaNGA 8313-1901

Photometric data from the DESI Legacy Imaging Surveys
+ spatially resolved spectroscopic data from the MaNGA survey

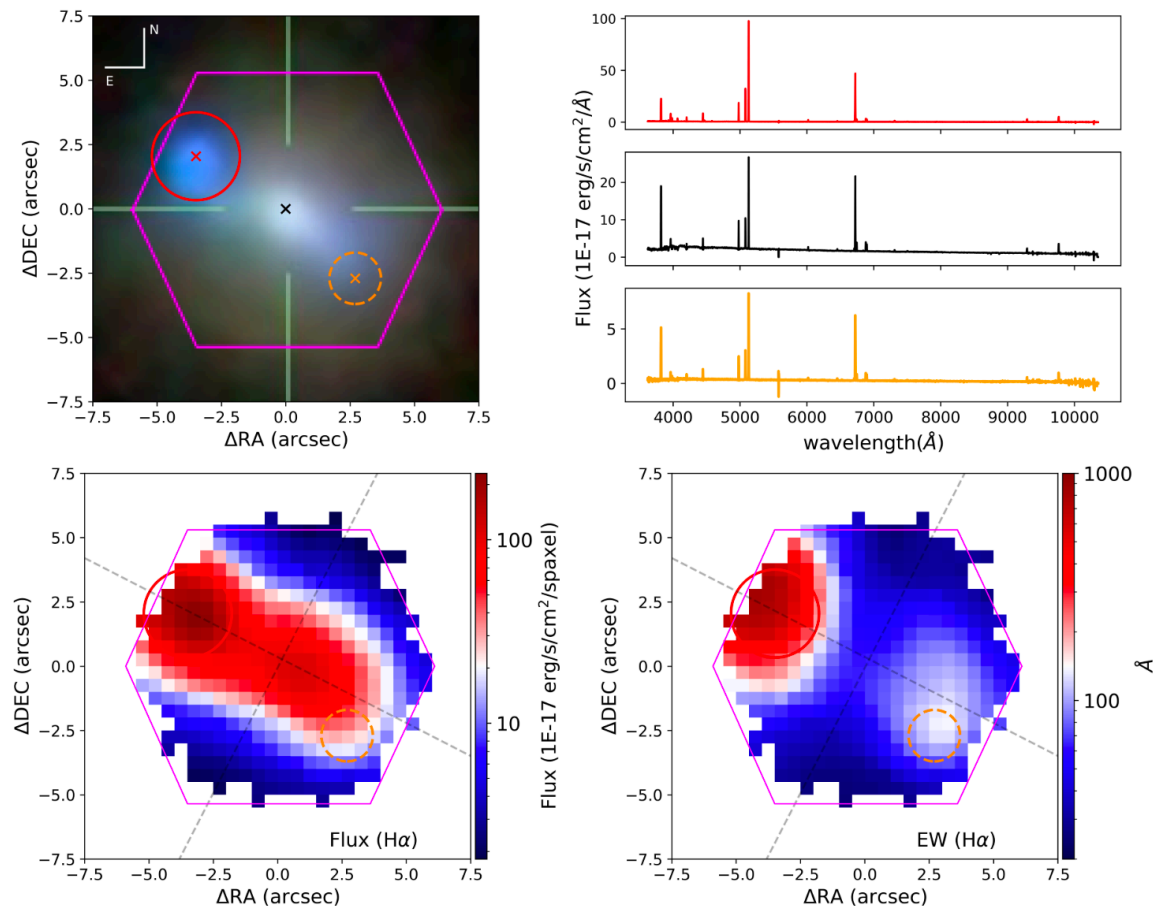


Figure 1. The top left panel shows the SDSS *gri* composite image, which covers $15'' \times 15''$ in size and corresponds to $7.56 \text{ kpc} \times 7.56 \text{ kpc}$ at its distance. The magenta hexagon shows the coverage of the MaNGA bundle in this field. The red solid circle and the orange dashed circle are the locations of the NE clump and the SW clump, defined in Section 3.1 and 3.2, respectively. In the top right panel, the spectra of three spaxels indicated as red, black, and orange crosses in the top left panel are shown as the red, black, and orange solid lines, respectively. Bottom left: the dust-corrected flux map of the $\text{H}\alpha$ emission line. Bottom right: the Equivalent Width map of the $\text{H}\alpha$ emission line. The major and minor axes are shown as dashed grey lines. The position angle is adopted from the NASA-Sloan Atlas catalog.

Сильные эмиссионные линии во всех трех спектрах.
NE clump существенно более сильные, чем в центре.

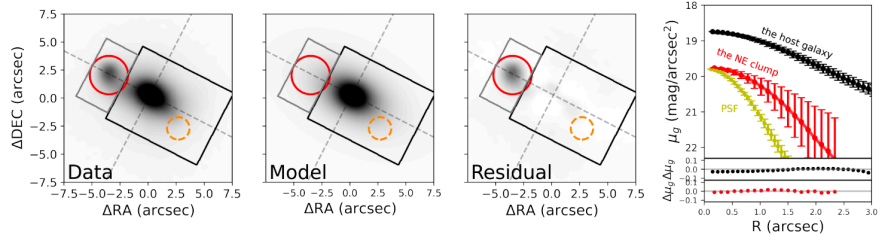


Figure 2. Two-dimensional surface brightness modeling of the host galaxy of MaNGA 8313-1901 with GALFIT. The leftmost panel shows the observed g -band image of BASS with a pixel size of $0.06''$ and a PSF FWHM of $1.68''$. The black box is defined to be the fitting area of the host galaxy. The grey box with a size of $\sim 3'' \times 6''$ and centered at the peak of H α flux in the NE clump is the region we fit to obtain the morphological parameters of the NE clump with a size of $\sim 3'' \times 6''$. The best-fitted 2D model of the host galaxy given by GALFIT and the host subtracted residual image are shown in the second and third panels. The color scale is the same for all images, and ranges from -0.25 to 20 nanomaggies/arcsec 2 . The two grey dashed lines show the major (northeast-southwest direction) and the minor (northwest-southeast direction) axes. In the left three panels, the red solid circle indicates our definition of the NE clump region with a radius of $1.71''$. The orange dashed circle with a radius of $1''$ shows our definition of the SW clump (Section 3.2). The rightmost panel shows the surface brightness profiles of the host galaxy (black), the NE clump (red), and the scaled PSF model (yellow). The dots with error bars demonstrate the observed data, and the lines stand for the 1D profiles of the best-fit GALFIT model. The two bottom sub-panels of the rightmost panel are the residual ($\mu_{\text{data}} - \mu_{\text{model}}$) profiles of the surface brightness of the host galaxy (black) and the NE clump (red) respectively.

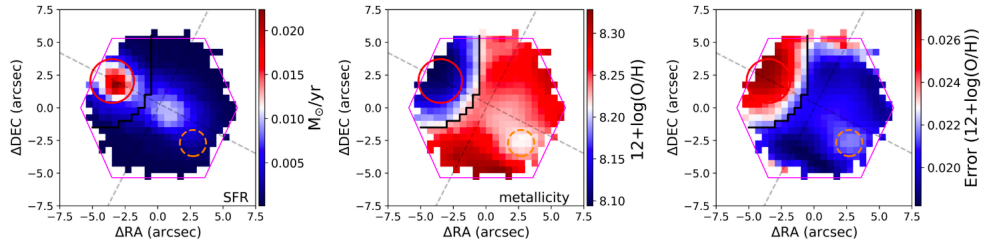


Figure 3. The SFR map (the left panel) and the metallicity map (the middle panel) with the metallicities measured via the O3N2 method. The error map of the metallicity measurements is shown in the right panel. The red circle indicates the NE clump region, and the orange dashed circle shows the SW clump region.

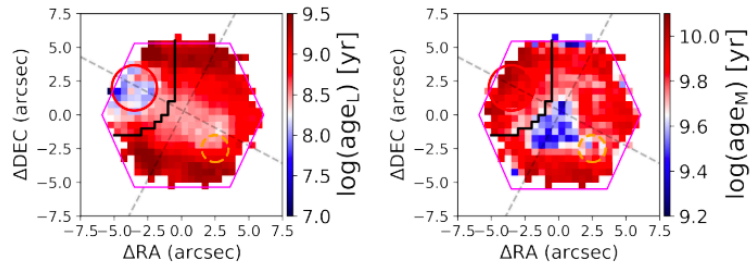


Figure 4. The maps of the light-weighted stellar age (the left panel) and the mass-weighted stellar age (the right panel).

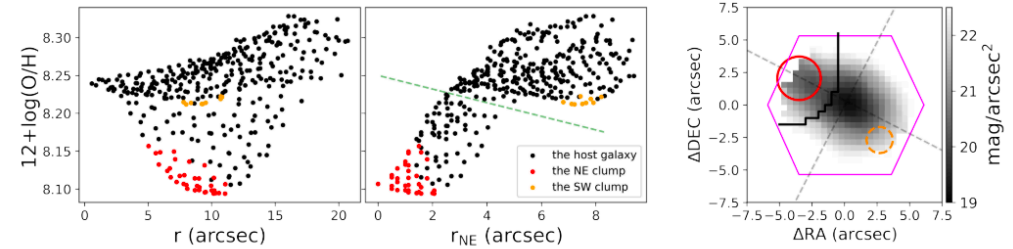


Figure 5. Left: The radial distribution of metallicity for every MaNGA spaxel. Middle: The offset metallicity radial distribution. The radius is defined as the distance to the spaxel with the highest H α flux in the NE clump. There are two branches in this panel, well separated by the green dashed line. Right: The g -band image from the MaNGA survey. The red circle is the NE clump region, and the orange dashed circle shows the SW clump region. The black line is a dividing line of spaxels located between the two branches shown in the middle panel. The red, orange and black data points in the left panel and the middle panel represent the spaxels in the NE clump, the spaxels in the SW clump, and all other remaining spaxels in the right panel, respectively.

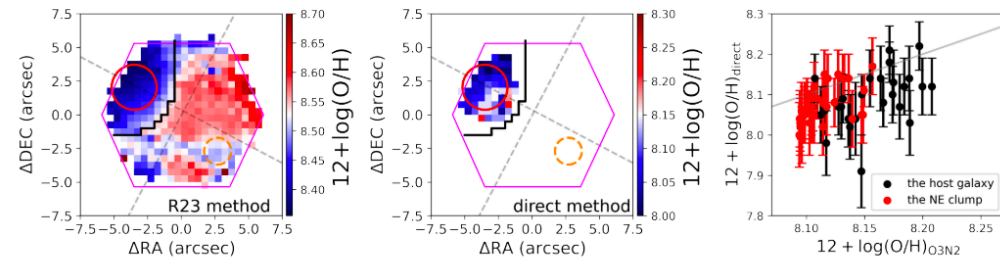


Figure 6. Left: The metallicity map obtained via the R23 method. Middle: The metallicity map obtained via the direct T_e method. Only 61 spaxels with significant [O III] λ 4363 detections ($S/N > 5$) are shown. Right: The comparison between the metallicities obtained from the direct method and those obtained from the O3N2 method for the 61 spaxels in the middle panel. The red data points and the black data points represent the spaxels inside and outside the morphologically defined NE clump (the red circle in the middle panel), respectively. The grey line is the one-to-one correlation.

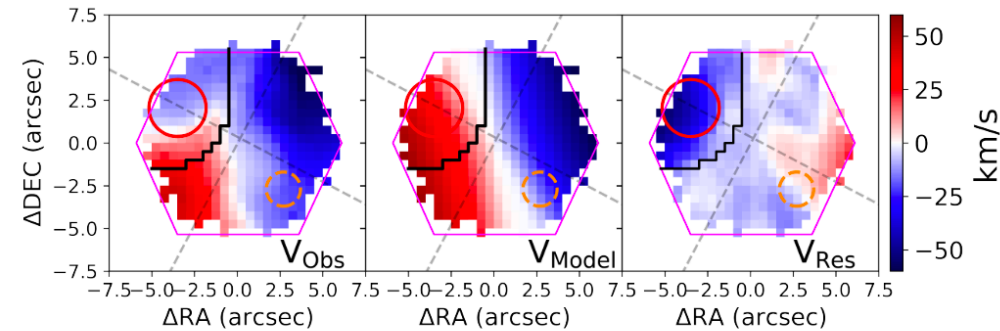


Figure 7. The observed H α velocity map (the left panel), the best-fit rotation model for the host galaxy (the middle panel), and the residuals ($V_{\text{obs}} - V_{\text{model}}$) of the H α velocity field (the right panel) of MaNGA8313-1901.

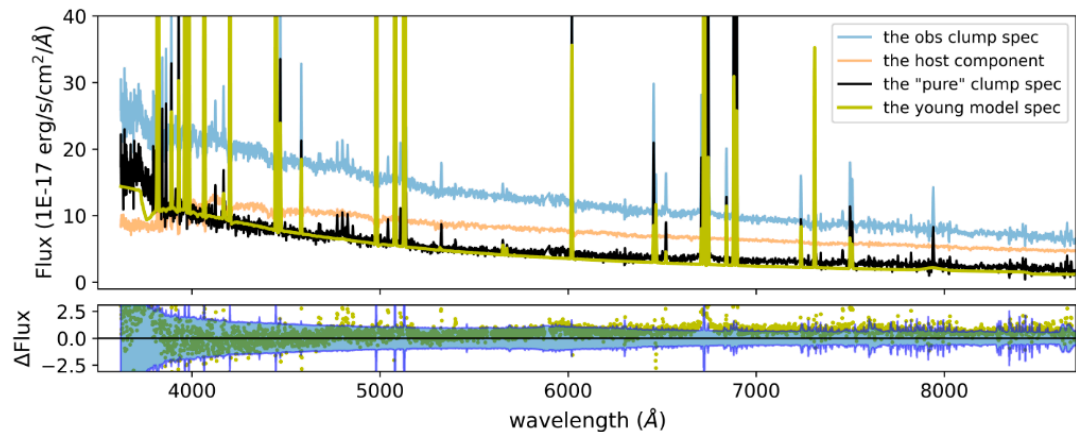


Figure 8. The spectra of different components in the NE clump of MaNGA 8313-1901. In the upper panel, The observed spectrum in the NE clump is shown in light blue. The light orange line represents the estimated host component in the NE clump. The “pure” clump spectrum, i.e., the observed clump spectrum (light blue) subtracted by the estimated host spectrum (light orange), is shown in black. The yellow dashed spectrum shows the modeled clump spectrum constructed by `Prospector` (see text for details). The residual of the modeled “pure” clump spectrum, i.e., the difference between the “pure” clump spectrum and the modeled one, is shown in the lower panel. The blue shaded area shows the 3σ error region of the observed spectrum.

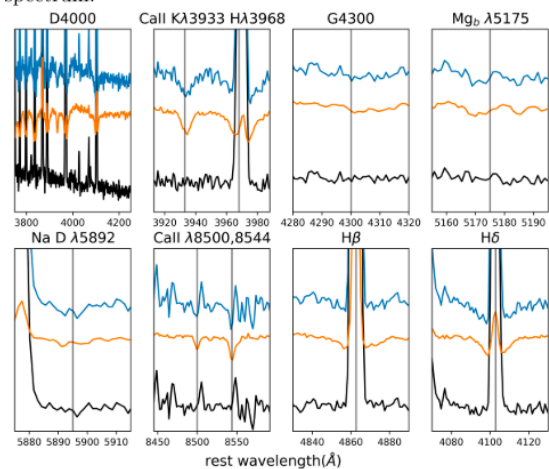


Figure 9. The zoom-in spectra of the observed spectrum (the blue line), the host component spectrum (the orange line), and the “pure” clump spectrum (the black line). From top left to bottom right, we show the D4000 absorption lines, Ca II λ 3933, 3968, G 4300, $Mg_b \lambda$ 5175, NaD λ 5892 and Ca II λ 8500, 8544, and emission lines $H\beta$ and $H\delta$.

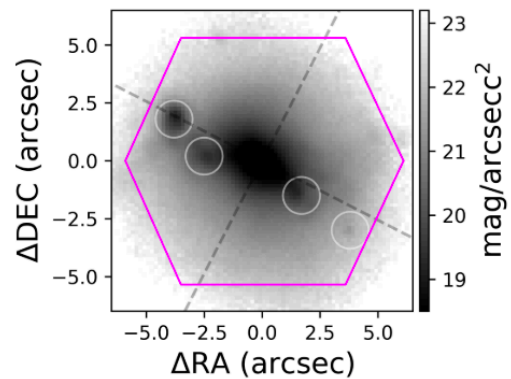


Figure 10. The i -band image of HSC survey. We draw four white circles to highlight the small knots that we find.